

See discussions, stats, and author profiles for this publication at: <https://www.researchgate.net/publication/265548193>

In search of ideal knots

Article in *Computational Methods in Science and Technology* · December 1998

DOI: 10.12921/cmst.1998.04.01.09-23

CITATIONS

73

READS

882

1 author:



Piotr Pieranski

Poznań University of Technology

52 PUBLICATIONS 1,653 CITATIONS

SEE PROFILE

CHAPTER

IN SEARCH OF IDEAL KNOTS

PIOTR PIERAŃSKI
Department of Physics
Poznan University of Technology
Piotrowo 3, 60 965 Poznan, Poland
and
Institute of Molecular Physics,
Smoluchowskiego 17, 60 159 Poznan
E-mail: pieransk@phys.put.poznan.pl

A particular version of the knot tightening algorithm is described. It is shown that the algorithm is able to remove empty loops and nugatory crossing leading to the simplification of the conformation of any knot. The problem of finding the ground state conformation of knots is discussed. Results of tightening various types of knots are presented and analysed.

1 Introduction

Knot is a closed, selfavoiding curve. From the topological point of view all conformations of the curve accessible via transformations during which no self-crossings occur are equivalent. From the point of a physicist, who thinks of the knot as a material object, whose points interact with forces stemming e.g. from a certain potential field, different conformations of a knot may have different energies. In such a case finding the ground state of the knot, i.e. the particular conformation at which the internal interaction energy reaches its minimum, is a challenging task. Our interest in the problem was stimulated by the seminal paper on the energy spectrum of knots and links by Moffat¹. A rigorous treatment of various formulations of the energy function and references concerning the history of the problem can be found in chapters by O'Hara and Diao et al. in this volume. Here, we shall limit ourselves but to the simplest case of the energy defined by the knot thickness. Putting aside all subtleties of the definition, one can state that the scale invariant parameter which determines in this case the knot energy (in what follows we shall refer to it as the *thickness energy*) is the ratio L/D , where L is the length of the rope (or tube) used to tie a particular conformation of the knot and D is the diameter of the rope.

The conformation at which the L/D parameter reaches its global minimum is the *ground state* of the knot. Knots in their ground state conformations are sometimes called *ideal* - term coined by Stasiak². As it happens with ideal things, to

reach ideal conformations of knots is not a trivial task: as we have found out, some of the ideal knots presented in Ref. 2 are in fact not ideal - we managed to find conformations for which values of the L/D parameter are smaller. But, are the values we managed to find *the minimal ones*? We cannot be sure. Thus, talking below less about the ideal knots we shall talk more about the tool we created to search for them.

2 The knot inflation process

Let K be a given knot type. Let C_K be a particular, smooth conformation of the knot at each point \mathbf{r} of which the tangent unit vector \mathbf{t} is well defined. Imagine now a process in which the curve C_K is slowly inflated into a tube T_K . At each point \mathbf{r} of C_K the cross-section of the tube with a plane perpendicular to the tangent vector \mathbf{t} is a disk of diameter D . If the curvature all along C_K is finite and smaller than a certain critical value, depending on the actual value of D , the tube the inflation process starts without problems. Depending on the actual shape of C_K , overlaps between different segments of the tube, or at its strongly curved parts, will soon appear. If by an appropriate procedure modifying the shape of C_K (keeping its length L fixed) the overlaps are removed, the process of inflation can continue until the conformation of the knot reaches a limit state above which the newly created overlaps can no more be removed.

The knot inflation process was introduced independently by a few authors^{1,3,4,5}. As easy to guess, instead of inflating the tube while keeping its length fixed, one can consider the complementary process in which the length of the tube is reduced while its diameter is kept fixed. Below we present the Shrink-On-No-Overlaps (SONO) algorithm we developed during our studies of braids⁶.

Our approach to the knot tightening process is experimental. It was not our aim to create a universal, autonomous algorithm able to find on its own the global ground state conformation of any knot. What we were aiming at was rather the creation of a virtual laboratory within which various experiments on knots could be performed, among them - tightening. The SONO algorithm is one of the tools found in the virtual laboratory. Other tools allow one to study various properties of the knots such as their curvature and twist maps, writhe and the average crossing number.

It is interesting that laboratory experiments with tightening knots tied on a real rope of have been performed not by physicists but mathematicians. The experiments are described in Ref. 4.

3 Shrink-On-No-Overlaps (SONO) ALGORITHM

Shrink-On-No-Overlaps algorithm is built from a number of procedures. Below we describe them one by one. Developing the SONO algorithm we tried to make it as fast as possible, thus simplicity of the applied procedures was of primary importance.

3.1 *ControlLeashes (CL) procedure.*

For obvious reasons, in the numerical experiments described below knots are discretised. Thus, let P_i , $i=1..N$, be equidistant points belonging to C_K . In what follows we shall refer to them as the *nodes*. $l=L/N$ denotes the length of *leashes*, which tie neighbouring nodes along the knot. The length of all leashes should be equal l . To keep an eye on it we defined a ControlLeashes procedure. It checks the distance $d_{i,i+1}$ between i and $i+1$ node and corrects its length to the proper L/N value.

If $d_{i,i+1} \neq l$ then nodes i and $i+1$ are symmetrically moved (away or towards their centre of mass) along the line which passes through them to positions at which $d_{i,i+1}=l$.

The procedure starts at a randomly chosen node and runs, accordingly to another random choice instruction, up or down around the chain of nodes. Obviously, the CL procedure defined in such a manner is not selfconsistent; after its single application the leashes are not of equal length. On the other hand, it is also obvious that its frequent application should reduce the dispersion of the leash length. It does.

The CL procedure returns the lengths of the longest and shortest leashes found within the chain. Monitoring the values one can estimate the actual dispersion of the leash lengths.

3.2 *FindNeighbours(FN) and RemoveOverlaps (RO) procedures*

Nodes are points. To simulate a tube of diameter D we assume that each of the points is surrounded by a hard sphere of diameter D . As the number N of the nodes is large (or L is small) and the leash length l is smaller than D , the spheres surrounding consecutive nodes must be allowed to overlap. To achieve the aim, the hard core repulsion between spheres is defined in a particular manner: the spheres repel each other only if their index distance is larger than a certain *Skipped* integer.

The *index distance* between an i -th and k -th node is defined as the (smaller of the) number of leashes which separate nodes in question along the chain. A proper choice of the *Skipped* parameter is crucial. It should be larger than $\text{round}(D/l)$. One

should take into consideration situations in which the simulated tube makes the tightest U-turn

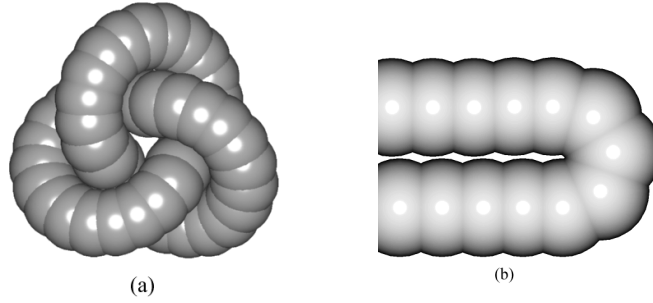


Fig. 1 (a) The discrete form of the 3.1 knot as seen by the SONO algorithm. The number of nodes $N=49$ is about 3 times smaller than the normalised standard value $\text{round}(10L/D)$. (b) The tight U-turn.

The sphere located at the entrance to such a U-turn should be blind to overlaps with all spheres found within the turn and it should start repelling all spheres which left the turn. Since the length of the tightest U-turn equals $\pi D/2$, the proper *Skipped* value should be close to $\text{round}(\pi D/2l)$.

Removing overlaps which appear in the knot during its tightening process is the most time consuming task. If the procedure which performs it is defined without imagination, its time consumption grows with N^2 . This happens if at each step of the tightening process possible overlaps of each node with each other node are checked. If the knot tightening process is slow, the evolution of the knot conformation is smooth and uniform and for a given node only a few nodes have a chance to overlap with it. (By a node we mean here the sphere which surrounds it.) Thus, before the overlap removing procedure is called, one should find for each node all nodes which have a chance to overlap with it. This task is performed by a FindNeighbours (FN) procedure which updates an integer array $\text{nn}[1..N, 1..m]$, whose i -th row contains indexes of all nodes which are found within a distance smaller the $(D+\epsilon)$, where ϵ is a small parameter adjusted experimentally. At the entrance to the FN procedure the nn array is zeroed. Then, consecutive rows are filled in. If the length m of the rows is chosen large enough, at the end of the FN procedure the rows are found to be only partially filled in: they end with sequences of zeros.

Assume that the nn array has been updated. Then, the RO procedure starts detecting and removing overlaps. The check starts at a randomly chosen nodes and, according to another randomly chosen parameter, it runs up or down the chain of nodes. For a given i -th node only the nodes whose indexes are found within the i -th row of the nn array are checked for overlapping. If the spheres surrounding the i -th and j -th nodes are found to be overlapping, the nodes are shifted apart,

symmetrically, along the line which joins their centres, to a distance $(D+\delta)$, where δ is another experimentally adjusted parameter. Putting $\delta>0$ leaves some extra free space between the shifted apart spheres. As found experimentally, this speeds up the tightening process.

The FN procedure is called much less frequently than the CL and RO. Typically it is called only every 200 iteration steps. As in the case of the CL procedure, the RO procedure is not selfconsistent. Removing overlaps between two nodes may create overlaps with other neighbours of the moved nodes, however, repeated use of the procedure asymptotically removes all overlaps (if the knot is not too tight already). The state of overlaps found within the chain is monitored by finding during the run of the RO procedure the values of the maximum and average overlaps.

3.3 *ShiftNodes (SN) procedure.*

As stated at the beginning, in the numerical experiments knots are represented by knotted, discrete chain of spherical beads threaded on C_K . Since the beads are spherical, the surface of the chain is not smooth. To avoid jamming we introduced into the SONO algorithm an additional procedure which shifts the beads along the C_K thread by an incommensurate fraction of the internode (leash length) distance, left or right. New positions of the beads are calculated via a simple, linear interpolation. The primary aim of the shifting procedure is to prevent jamming. Its sideeffect, which proved to be of great importance, is smoothening and cutting corners of C_K . The latter leads to some additional effects such as a rotation of the knot as a whole, which happens in the case of strongly chiral knots, e.g. the 3.1 knot.

3.4 *ReduceNodeNumber (RNN), DoubleNodeNumber (DNN) and NormalizeNodeNumber (NNN) procedures.*

Tightening a knot aimed at finding its global ground state is a difficult experiment. It aims at minimising $\Lambda=L/D$ vs. C , where C denotes the actual conformation of the knot. Unfortunately, for most knots the $\Lambda(C)$ function displays a whole set of local minima. Any procedure aimed at finding the global minimum must be able to get out of them. In the thermal bath based Monte Carlo algorithms such as that used in Ref. 2, thermal fluctuations perform the task. In the mechanical knot tightening process simulated with the SONO algorithm the mechanism is different. Experiments prove that reduction of the number of nodes and increasing the δ parameter in the RO procedure allows one to cross some of the minima. We defined simple procedures which reduce twice (RNN) or double (DNN) the number of

nodes. The procedures are called, when necessary, by the operator performing the tightening experiment.

To obtain comparable accuracy of parameters for different types of knots, we defined also a procedure (NNN) which normalises the node number to a common standard value depending on Λ . In all experiments described below we assumed that the standard number of nodes is equal $\text{round}(10 \cdot \Lambda)$. This particular choice of the standard node number is of course arbitrary.

In addition to the procedures described above the numerical knot tightening workbench contains: procedures finding the total length L of the knot, its writhe Wr and the average crossing number ACN , the procedure finding and plotting the curvature map τ and, finally, the procedure which plots the actual conformation of the knot. Images of the knot conformation are stored on the hard disk what at any step of the tightening process allows the operator to call an animation procedure which displays the images in form of a short movie. Analysing the movie the operator may estimate the effectiveness of the tightening process and check if the knot did not change its type.

3.5 *The core of the SONO algorithm.*

The general flow diagram of the SONO algorithm is as follows.

1. The (x,y,z) coordinates of the nodes of a chosen knot are taken either from the procedure in which the knot is drawn with the mouse on the screen (the over- and undercrossings marked during the drawing process with mouse keys) or it is read from a file within which the coordinates were stored at one of the previous runs.
2. The nn array containing indexes of the near neighbours is filled in with by the FN procedure.
3. The lengths of the internode leashes are corrected by the CL procedure.
4. Overlaps are removed with the RO procedure.
5. If the average overlap value is smaller than a certain (defined by the operator) threshold, the knot is tightened: the (x,y,z) coordinates of the nodes and the leash length l are multiplied by a scaling factor $s < 1$, while the diameter D determining the overlapping remains unchanged.

Steps 3, 4 and 5 are repeated NumOfIt times, NumOfIt being of order $10^2 - 10^3$, before the FN procedure used in step 2 is called again.

4 TESTS OF THE SONO ALGORITHM

4.1 *Untangling an entangled unknot.*

Any procedure aimed at searching for the global ground states of knots should be able to perform such basic tasks as removing empty loops and nugatory crossings from even the most entangled conformation of a knot. Fig. 2 demonstrates how the SONO algorithm performed the task in the case of an entangled conformation of the trivial knot.

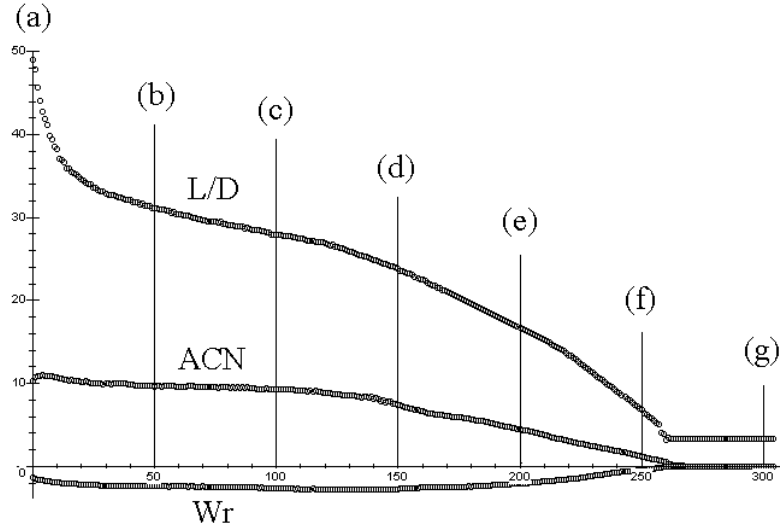


Fig. 2 Consecutive stages of the tightening process performed by the SONO algorithm on an entangled trivial knot. The run presented in the figure lasted about 5 min. on a PC Pentium 100.

In spite of its apparent effectiveness the SONO algorithm performs the untangling task in a rather awkward manner. Rather than tediously pulling out the empty loops it should just detect and cut them. Such a CutEmptyLoops procedure may be added to the tools it uses.

4.2 *The Moffat test*

Another test of knot tightening algorithms was suggested by Moffat. As he put it in his comment⁷ to Ref. 1: "It would be interesting to test the algorithm on the simpler $T_{3,2}$ and $T_{2,3}$ configurations of the trefoil; it is not clear to me, how $T_{3,2}$ could flow to $T_{2,3}$ through the process described."

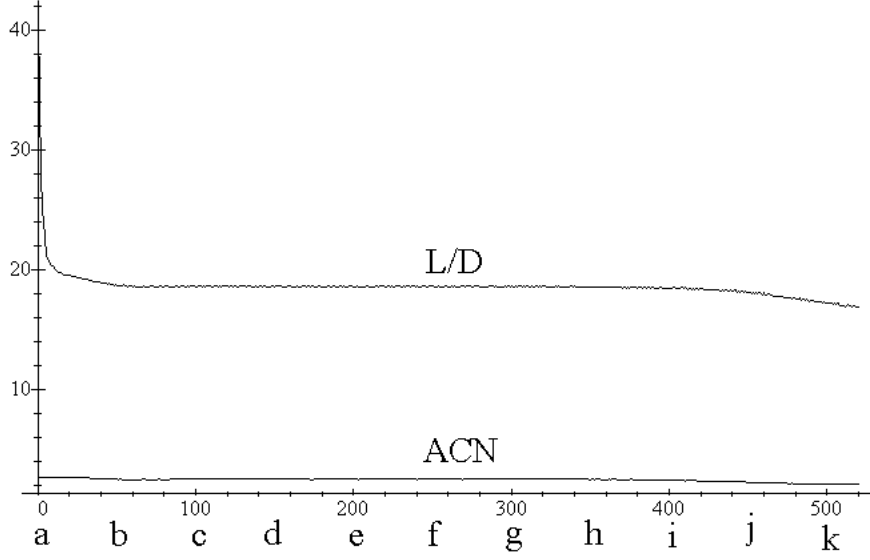


Fig. 3 Moffat test of the SONO algorithm. (a) the initial, loose conformation of the $T_{3,2}$ knot generated numerically. (k) the ground state configuration.

Fig. 3 presents result of the Moffat test we performed with the SONO algorithm. A symmetrical $T_{3,2}$ initial configuration (a) was generated numerically. Then, the configuration was read by the SONO algorithm and tightened. As clearly seen in the figure, after the very rapid initial stage, in which the loose initial configuration became tight (b), the evolution practically stops. The L/D and ACN parameters remain on average constant: a local minimum or saddle of the knot energy has been reached. However, as seen in the figure as well, the L/D value fluctuates. The fluctuations are induced mostly by the ShiftNodes procedure; let us remind that the discrete representation of the knot is not smooth, see Fig. 1. As a result of the fluctuation the symmetry of the $T_{3,2}$ configuration becomes broken (h), and the knot slips into the ideal $T_{2,3}$ configuration. Let us note that the time needed to break the symmetry of the $T_{3,2}$ configuration strongly depends on the number of nodes. A considerable, temporary reduction of the number allows the operator to initiate it. During the run presented in the figure all parameters of the SONO algorithm remained fixed. We performed the Moffat test for other torus knots. In all studied cases the SONO algorithm managed to break the n -fold symmetry of the $T_{m,n}$ knot.

4.3 The Perko Pair test

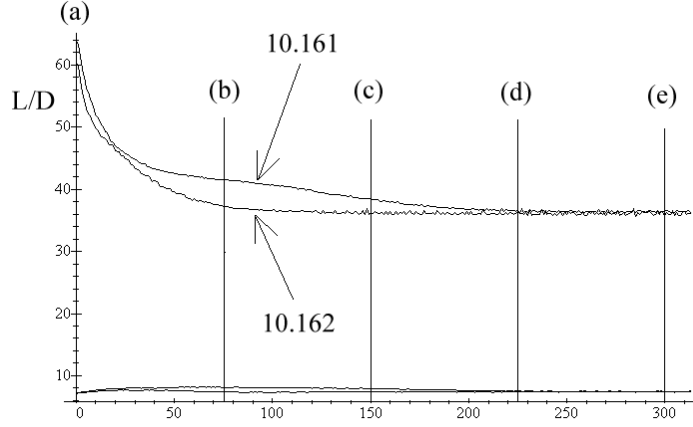


Fig. 4 Evolution of knots from the Perko pair to the identical final conformation.

Another test, which any algorithm aimed at finding the ideal conformations of prime knots should pass is the ability to bring knots 10_{161} and 10_{162} , the Perko pair, to a single, minimum energy conformation. The test was passed by the tools used in Ref. 2. In chapter by Stasiak et al. we presented how the task of bringing the Perko pair knots to the same conformation was performed by the SONO algorithm.

Initial conformations (a) of the Perko pair knots were defined by redrawing on the screen the conformations found in „*The Knot Book*” by C. C. Adams, p.32. The conformations were tightened separately with the SONO algorithm. Fig. 2 presented in chapter by Stasiak et al. shows consecutive stages of the knots evolution. As checked by an additional knot comparing procedure, although differently oriented, the final conformations of the knots were identical.

Fig. 4 presents the evolution of L/D for both knots. As seen in the plot, it is rather the 10_{161} knot which has a problem with finding the proper shape; evolution of the 10_{162} knot is rapid and leads immediately to the final conformation.

5 In search of ideal prime knots

First pictures of the ideal prime knots were presented in Ref. 2. As mentioned above, tests we performed with the SONO algorithm revealed that some of the configurations presented were not ideal.⁸ Below we present a numerical experiment which illustrates well the problems encountered during the search for the ideal conformations.

The first, most spectacular case is the 5_1 knot. Its conformation presented in Ref. 2 has a 5-fold symmetry axis and $L/D=24.2$. SONO algorithm managed to break the symmetry arriving at a conformation for which $L/D=23.5$. Fig. 5 presents the

symmetry breaking process observed in a single run lasting on a PC 100MHz about 2 min. The run started from a symmetrical $T_{2,5}$ conformation generated numerically (a). Initially, (a) - (c), the evolution was very fast until the knot became tight (c). Then, the evolution stopped (c), (d), (e) - the knot entered a local energy minimum. The stable tight conformation preserves the 5-fold symmetry axis present in the initial conformation. To induce the symmetry breaking, the δ parameter which determines the distance to which the overlapping nodes are shifted by the RO procedure was temporarily increased to 0.1 (previously it was equal 0.00001). This resulted in strong fluctuations of the knot conformation visible within the L/D plot. Figures (f), (g), (h), (i) present evolution of the knot shape towards the asymmetrical conformation (j).

Obviously, the knot conformation (j) to which the SONO algorithm arrived in the single run described above is not of a good quality. First of all, the number of nodes, $N=46$, of which it is built is too small to provide reliable values of its L/D , ACN , Wr parameters. In a standard procedure we apply to clean knots, its node number is normalised to $\text{round}(10*L/D)$ and the overlaps are carefully removed. We do not describe the cleaning procedure in more detail, although its application is quite essential if reliable data are to be obtained.

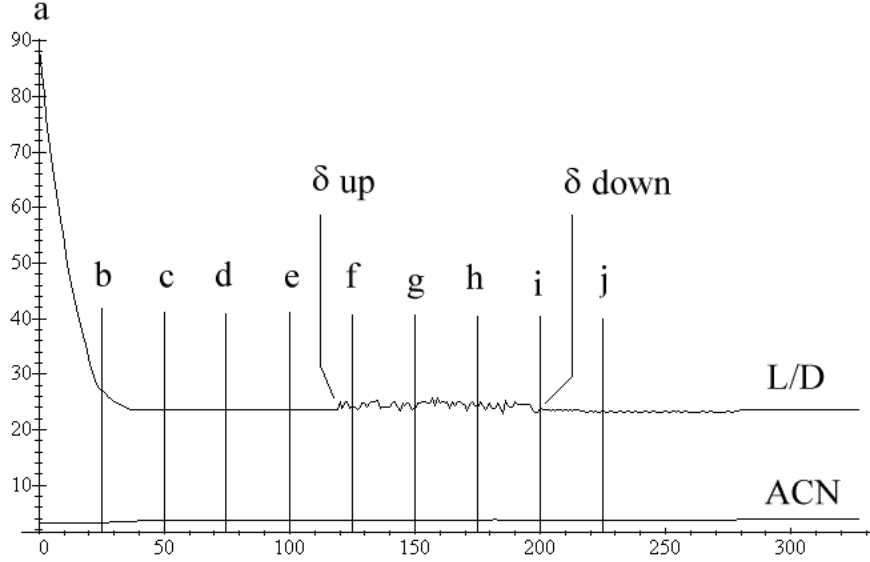


Fig. 5 Symmetry breaking of the 5_1 torus knot observed during the tightening of the knot with the SONO algorithm. See text.

The local minimum encountered during tightening of the 5_1 knot has been found also in the case of larger $T_{2,m}$ knots (m_1 knots in the Rolfsen classification). The Pascal code we are using allows us to study $T_{2,m}$ knots up to $m=63$.

The case discussed above clearly demonstrates that the knot inflation process may encounter problems when getting into the local minima within the thickness energy function. On the other hand, the case demonstrates also that the tools built into the SONO algorithm may in some cases allow the operator to force the knot to leave them. In the end, however, we cannot be sure if the conformation to which the knot eventually arrives is the final one, i.e. if the global energy minimum was reached. At the present state of the art of tightening knots we must admit that we have no certainty if the conformations to which we arrived are the ideal ones. On the other hand, due to the clear definition of the thickness energy the conformations obtained can be compared: the lower L/D , the better.

5.1 Prime knots up to 9 crossings.

The race for the lowest thickness energy conformations was initiated with the Monte Carlo annealing procedure whose results were presented in Ref. 2. The best conformations to which we arrived applying the SONO algorithm to all knots up to 8

crossings are shown in the Plates 1-3. L/D , ACN and Wr parameters of the conformations are listed in Table I found in chapter by Stasiak et al. Here we present two plots covering a slightly larger range of knots.

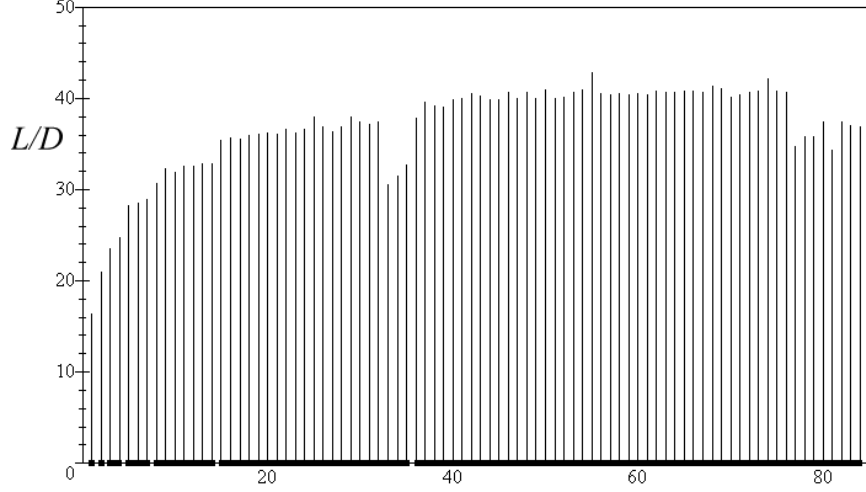


Fig. 6 The thickness energy for consecutive knots up to 9 crossings. Thickness energy is plotted in units of the rope diameter D .

The first one, Fig. 6, analogous to Fig. 2 found in Ref. 4, presents the L/D values of the consecutive prime knots up to 9 crossings in the order they are listed in the Rolfsen table. In the terminology of Ref. 3, the plot presents the *closed thickness energies* in units of the rope diameter D .

Note the drop, visible in Fig. 6, in the L/D value as the nonalternating knots are reached in classes of both 8 and 9 crossing knots.

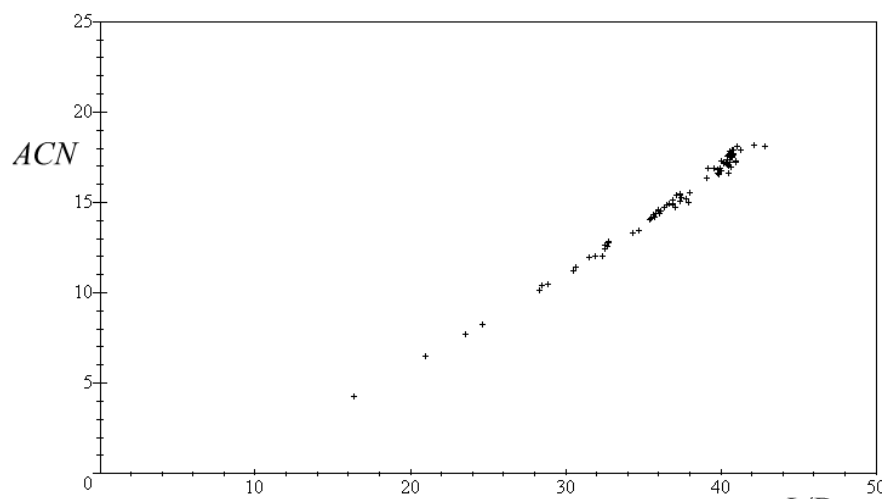
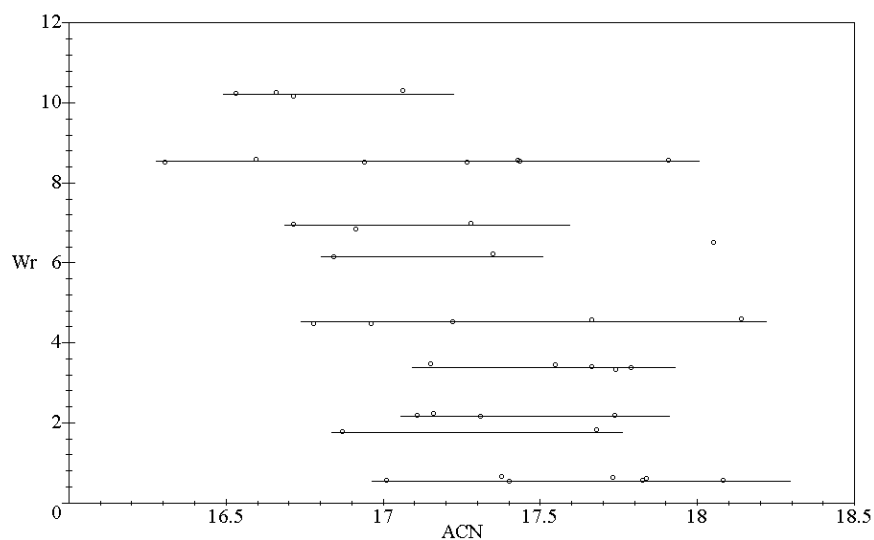
Fig. 7. Average crossing number ACN of prime knots up to 9 crossings vs. L/D .

Fig. 8. Writhe vs. average crossing number for all 9 crossings knots.

The second plot, Fig. 7, follows the idea presented in Ref. 2 and correlates the L/D values with the average crossing number ACN . Note, that the L/D vs. ACN relation, apparently linear at the beginning, is clearly nonlinear in a larger interval.

Trying to find the quantitative description of the relation we studied larger torus knots $T_{2,m}$, which in the Rolfsen notation are denoted as m_1 knots, m - odd. The nonlinearity of the ACN vs. L/D relation is clearly visible in Fig. 5 found in chapter by Stasiak et al., where we plotted data of all knots we studied.

Another essential parameter which characterises optimised conformations of knots is their writhe. Fig. 8 presents the variable correlated with the average crossing number. As clearly seen in the figure, the writhe is a variable, which within a family of knots with the same minimal crossing number takes values localised near a few, well defined levels. Reasons for this quasiquantization of writhe is not clear to us. For a discussion of the writhe vs. minimal crossing number correlations see chapter by Stasiak et. al.

Another problem, which puts in doubt the idea of using the parameters of the ideal conformations as the knot type identifiers, is the existence of knots which being of different type have almost identical values of their L/D , ACN and Wr parameters. This is well seen in the class of knots with $MCN=9$. Table 1 below presents values of the parameters for two pairs of knots for which the differences are smallest.

| Knot type | | L/D | | ACN | | Wr | |
|-----------|----------|-------|-------|-------|-------|-------|-------|
| 9_6 | 9_{16} | 39.97 | 40.00 | 16.87 | 16.77 | 10.26 | 10.19 |
| 9_{18} | 9_{23} | 40.71 | 40.58 | 17.48 | 17.47 | 8.57 | 8.56 |

Table 1 L/D , ACN and Wr parameters of two pairs of the most similar knots.

The differences are below the estimated accuracy of 1% with which the L/D , ACN and Wr parameters are determined. (In the table the values are given with excessive accuracy.) We are thus forced to conclude, that in practice the set of L/D , ACN and Wr values does not determine in an unambiguous manner the knot type.

5.2 Tightening of the torus knots $T_{2,m}$

To check the ACN vs. L/D dependence in a larger interval of L/D we tightened with the SONO algorithm the sequence of $T_{2,m}$ knots, m odd, which initiate in the Rolfsen notation all classes of knots with m crossings.

Initial configurations of the knots were generated numerically according to equations:

$$\begin{aligned}
 z(t) &= r(t) \cos(2\pi v_1 t), \\
 x(t) &= r(t) \sin(2\pi v_2 t), \\
 y(t) &= r(t) \cos(2\pi v_2 t), \\
 \text{where} \\
 r(t) &= R_0 + R_1 \sin(2\pi v_1 t);
 \end{aligned}$$

R_0 and R_1 are the radii of the torus onto the surface of which the knot trajectory is defined. Putting $v_1=2$ and $v_2=m$ one obtains circular conformation of the $(2,m)$ torus knots. In what follows we shall refer to them as the $T_{2,m}$ knots.

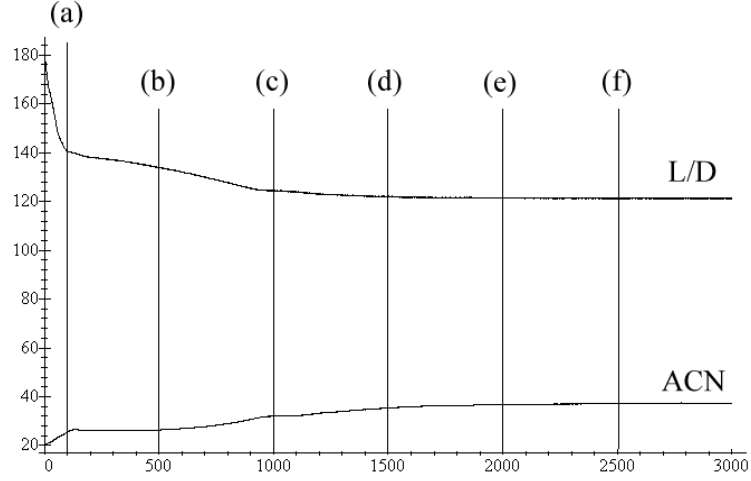


Fig.10 Evolution of the $T_{2,33}$ knot during the tightening process. See also Plate 4.

Evolution of the L/D and ACN parameters of the knot are presented in Fig. 10. For the sake of the clarity the tube of which the knot is made is drawn has a diameter equal $D/2$. The initial conformation of the knot is not shown. (a) presents the symmetrical conformation to which the initial conformation is rapidly tightened. As seen in (b) the SONO algorithm breaks it easily. In 8 places the arrangement of the tube becomes different. Fig 10. presents a fragment of the configuration in which 3 such places are well visible. The overall shape of the knot becomes almost octagonal; note that one side of the octagon is longer. This cannot be avoided, since the number of crossings is odd. This symmetry breaking leads to (c) - another typical conformation of the knot. The existence of the longer side leads to a another conformation of the knot (d), which eventually stabilises (e) and (f). Conformation of this type is characteristic to larger $T_{2,m}$ knots. Is it the ideal shape, or just one of the local minima? As stated in Chapter by Dubochet et al., we have found that there exists a better conformation. We discuss it in more detail in the next subsection.

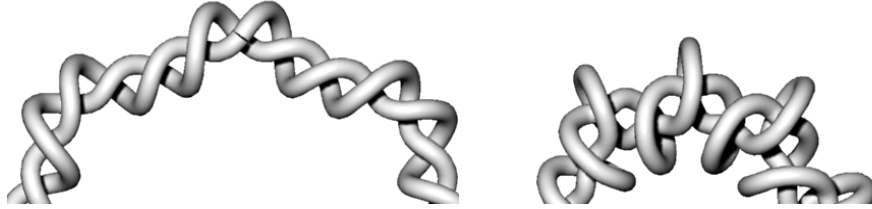


Fig.9 A typical arrangement of the tube in the $T_{2,33}$ torus knot in which the symmetry was broken.

5.3 Towards the ground state conformation of the $T_{2,m}$ knots

Tightening of large $T_{2,m}$ knots starting from their toroidal conformations leads to their compact, globular conformations. Experiments we performed prove that there exist better, with a lower L/D value, conformations of the knots. Fig. 11 present such a conformation of the $T_{2,33}$ knot.

As seen in the figure, structure of the initial conformation, from which the tightening procedure starts, is utterly different from the typical conformation of torus knots. In the conformation the tube is divided into two parts: the first one, bent into the a safety pin shape, forms the core around the second part of the tube is helicoidally wound.

The initial stage of the evolution process, during which all loose parts of the tube are shortened, is very rapid. In the next, much slower stage, the tightly packed safety-pin conformation becomes twisted. The rate of the twist is approximately the same in all torus knots and leads to a kind of a double-helix conformation. As noted by Stasiak⁹, the core part of the tube is not straight: under the pressure induced by the outer, helicoidal part it becomes helicoidally deformed as well. Analysis of the phenomenon lead us to formulate the following problem:

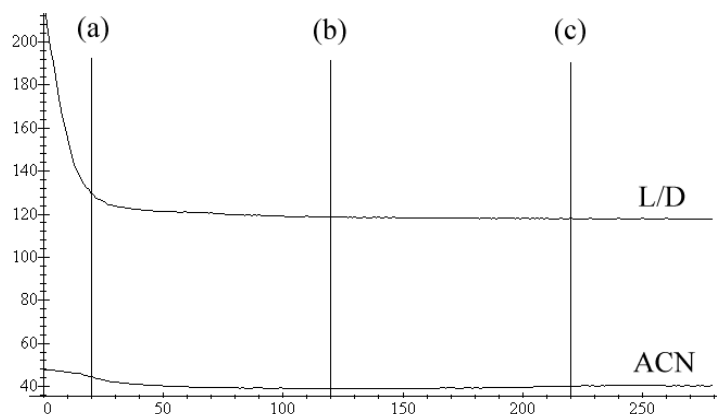


Fig.11 Evolution of the $T_{2,33}$ knot from the safety-pin initial conformation. The initial conformation is presented in a slightly different scale.

Which is the periodic conformation of two twisted together tubes, at which the L/D ratio reaches a minimum?

Answering the question may shed some light on the nature of the ground state conformation of the $T_{2,m}$ torus knots. In a different wording it asks how much of the tube we need to produce two crossings. The problem is being studied by Sylwester Przybył¹⁰. Fig. 12 presents four different conformations he considered.

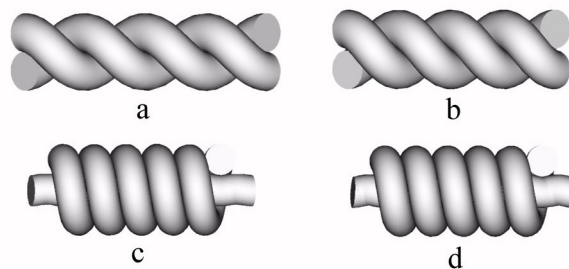


Fig. 12 Four closely packed conformations of twisted tubes. L/D per one period equals, respectively: (a) 8.886, (b) 8.5013, (c) 7.2261, (d) 7.2013. See text.

Let us describe in a few words the differences between them. All of the conformation can be described parametrically by two sets of equations:

$$\begin{aligned}
x_1(t) &= Pt & x_2(t) &= Pt \\
y_1(t) &= R_1 \sin(2\pi t) & y_2(t) &= -R_2 \sin(2\pi t) \\
z_1(t) &= R_1 \cos(2\pi t) & z_2(t) &= -R_2 \cos(2\pi t)
\end{aligned}$$

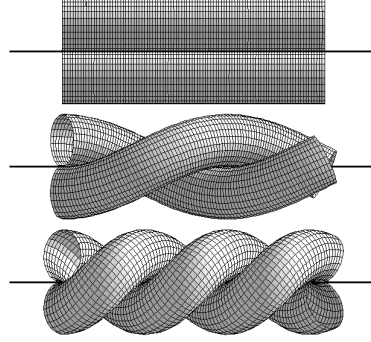


Fig. 13 The simplest way of twisting two tubes together. (a) Take two straight tubes and put them in parallel so that they touch along a common line. (b) Start twisting them together so that they remain in touch along the initial contact line. (c) Stop twisting, when the pitch of the structure equals π - overlaps are just about to appear.

In the first conformation, Fig. 13, the tubes are wound around and touch each other along the line lying between them: $R_1=R_2=0.5D$. The pitch of the periodic structure $P=\pi D$. The thickness energy per period $L_p/D=8.8858$. By L_p we denoted here the length of the tubes found within one period of the structure.

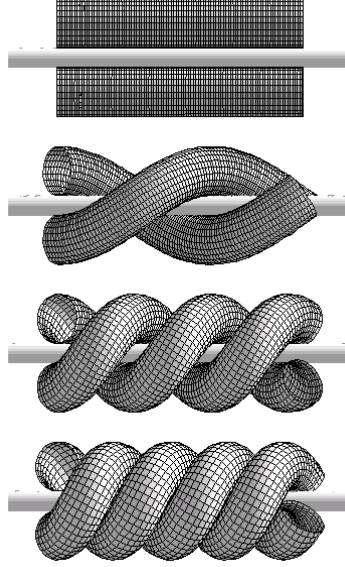


Fig. 14 The more clever way of twisting two tubes together. (a) Take two straight tubes and put them in parallel so that they do not touch. Insert a virtual cylinder between them. (b) Start twisting them together so that they remain in touch with the virtual cylinder. (c) Do not stop twisting when the pitch reaches the π value. (d) Stop twisting, when the tubes come in touch with each other. (Do not forget to remove the virtual cylinder.)

In the second conformation, Fig. 14. the radii of the spirals defining axial curves running inside the tubes are slightly larger than the radii of the tubes: $R_1=R_2=0.5229D$. As a result, a small hole appears along the x axis. The pitch of the structure is smaller than π : $P=2.6967D$. The tubes touch each other along two spiral curves running between the tubes. The thickness energy per period $L_p/D=8.5013$.

In the third conformation, Fig. 15, the radii of the spirals are different, but their sum is equal D : $R_1=0.97326D$, $R_2=0.0267D$. Pitch of the structure is much smaller than previously: $P=1.0136D$. The thickness energy per period $L_p/D=7.2261$. Note, that the value of R_2 is limited by condition that the curvature of the inner spiral cannot be larger than $2/D$.

In the fourth and it seems best, conformation (we do not show its construction details because visually it differs too little from the third one) $R_1=0.9670D$, $R_2=0.0377D$, thus, their sum is larger than 1. The minimal pitch $P=1.0139D$. The thickness energy per period $L_p/D=7.2013$.

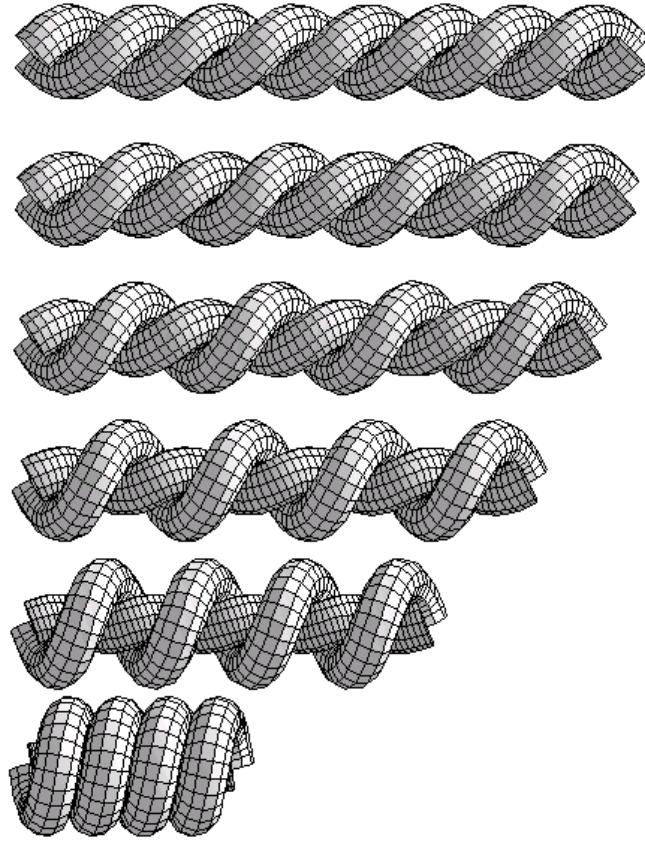


Fig. 15 Take the close packed structure obtained by procedure described in the caption of Fig. 13 and, remaining all time at the limit above which overlaps between the tubes appear, start increasing the radius of the spiral formed by one of the tubes decreasing at the same time the radius of the spiral formed by the other one. Stop the process, when the first spiral becomes close packed.

Looking at the numbers cited above, one can immediately see the reasons for which the m -fold symmetry of the initial conformations of the $T_{2,m}$ knots must be broken.

Conclusions

The simplest experimental procedure one can think of when trying to find the most tight conformations of a knot is to tie it on a rope and try to tighten it as much as possible by pulling the ends of the rope. To stay in agreement with what in mathematics is meant by a knot, one cannot forget at the end of the process to cut the spare parts and join the ends of the rope together.

The technique of numerical simulations provides us with a chance to perform such experiments in a much more clean manner:

- using the perfectly flexible and slippery, but at the same time perfectly hard in its circular crosssection rope,
- shortening the rope without the necessity of cutting it.

The SONO algorithm we described performs the simulation task in the most simple and thus effective manner. Using it we managed to find more tight conformations for a few from the knots considered in Ref. 2. Unfortunately, we cannot be by no means sure if the conformations we found are the most tight ones. What makes things even worse is that for the more complex knots results of the simulations depend on the initial conformations. We would be in a much better position if the ideal conformations of at least a few knots were known rigorously. (So far we know the rigorous solution but for a single knot – the trivial one.) We hope that mathematicians will be able to make some progress in this direction. Without a rigorous understanding of the nature of the ideal conformations the accuracy of results of any numerical work will remain unknown.

Acknowledgements

I thank Arne Skjeltorp for introducing me to the realm of knots. My work on the algorithm searching for the ground state of knots gained its proper intensity due to the friendly attitude of the Lausanne group: Jacques Dubochet, Andrzej Stasiak and Vsevolod Katritch. I thank LAU for the financial support.

The Pascal code of some of the procedures described in the paper was optimised due to help of Ben Laurie and Zdzislaw Michalski.

I thank Robert McNeel & Associates for providing me with the beta version of the *Rhinoceros* software, with the use of which most knot images presented within the text were created.

This work was carried out under KBN Project 8T11 F010 08p04.

References

-
- ¹ H. K. Moffat, 1990, The energy spectrum of knots and links., *Nature* **347**, 367-369.
 - ² V. Katritch, J. Bednar, D. Michoud, R. G. Sharein, J. Dubochet and A. Stasiak, 1996, Geometry and physics of knots., *Nature* **384**, 142-145.
 - ³ P. Pieranski, 1996, Search of ideal knots., *ProDialog*, **5**, 111 (in Polish).
 - ⁴ Y. Diao, C. Ernst, E. J. Janse Van Rensburg, this volume.
 - ⁵ A. Yu. Grosberg, A. Feigel and Y. Rabin, 1996, Flory-type teory of knotted ring polymers., *Phys. Rev.* **E 54**, 6618.
 - ⁶ P. Pieranski, S. Clausen, G. Helgesen and A. T. Skjeltorp, 1996, Nonlinear phenomena in systems of magnetic holes., *Phys. Rev. Lett.* **77**, 1620.
 - ⁷ H. K. Moffatt, 1996, Pulling the knot tight, *Nature*, **384**, 114.
 - ⁸ The tests were performed in close collaboration with the Lausanne group. I am gratefully obliged to Vsevolod Katritch who, at the time I started to work on prime knots, was already aware that some of the configurations he found were not the best one and whose remarks allowed me to clean the code of the SONO algorithm from numerous bugs.
 - ⁹ Private communication.
 - ¹⁰ S. Przybył, P. Pieranski, 1998, Search of ideal knots. III Application of Maple V.4 to the problem of two ropes tightly twisted together, *Pro Dialog* **6**, 18 (in Polish).